Research on Chemical Intermediates
https://doi.org/10.1007/s11164-020-04134-7

Design, in silico, one-pot synthesis, and biological evaluations of novel *bis*-urea analogs

Sajede Shoja, et al. ***[full author details at the end of the article]***

Received: 5 December 2019 / Accepted: 19 March 2020

Abstract

The structure of urea has received special attention due to its biological activity. A new and efficient one-pot three-component reaction for the synthesis of *bis*-urea compounds from a variety of substituted diamino derivatives and isocyanate derivatives at room temperature with suitable yield is reported. Seven novel *bis*-urea derivatives were designed, synthesized, isolated, purified, and characterized (**3a**–**g**) with a variety of aromatic and aliphatic linkers. All compounds were evaluated for their cytotoxic and antibacterial properties. Most of the synthesized compounds exhibited reasonable activity compared to the positive control group.

Graphic abstract

Development of a novel one-pot three-component reaction (3-CR) for the preparation of *bis*-urea scaffolds based on in silico studies was done. Evaluations of cytotoxic and antibacterial activities of all compounds were done. Most of the compounds exhibited good activities.

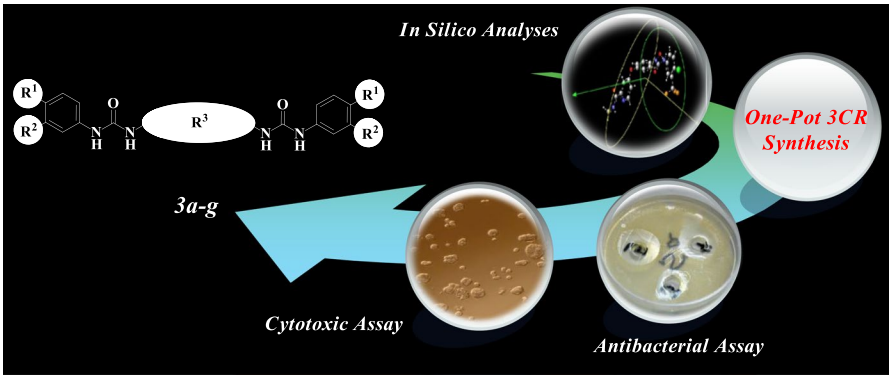

Keywords Synthesis · Design · Sorafenib · Cytotoxicity · Antibacterial · One-pot

Electronic supplementary material The online version of this article (https://doi.org/10.1007/s11164-020-04134-7) contains supplementary material, which is available to authorized users.

Published online: 02 May 2020

Introduction

One of the areas of interest in synthetic organic chemistry is finding suitable techniques for C–N bonding. It is widely used in natural product synthesis and industrial production [1, 2]. These functional groups are used as building blocks of several pharmaceuticals [3, 4] and agrochemicals [5]. Initial study indicates that the structure of urea is very important because NH groups can play an important role in forming hydrogen bonds with amino acids [6] and lead to its biological activity. Many urea analogs have also shown positive antiproliferative activity [7–10]. For example, sorafenib (*Nexavar*®), lenvatinib (*Lenvima*®), regorafenib (*Stivarga*®), and linifanib (*ABT-869*) include this functional group (Fig. 1).

Multicomponent reactions (MCRs) are considered as important methods in organic synthesis. These types of reactions have many advantages over conventional reactions such as higher chemical yields, operational simplicity, reduced purification and isolation processes and minimized time, energy, costs, and waste generation. MCRs are also valuable for the production of chemical libraries with a high diversity of bioactive compounds and high levels of molecular complexity. Thus, they help drug discovery programs to identify and optimize potential intelligent molecules [11–20].

Liver cancer is the sixth leading cause of cancer death in women and the second leading cause of cancer deaths in men [21]. Sorafenib (*Nexavar*®) is a diaryl urea multikinase inhibitor accepted by the FDA for the treatment for advanced hepatocellular carcinoma (HCC) in 2007 [22, 23]. It is also intended for testing other cancers, including clinical trials of brain, ovarian, leukemia, metastatic colorectal, glioblastoma, Hodgkin's lymphoma, metastatic breast, renal cancer, thyroid, non-small cell lung cancer (NSCLC), prostate cancers, melanoma, and bladder [24, 25]. Not only

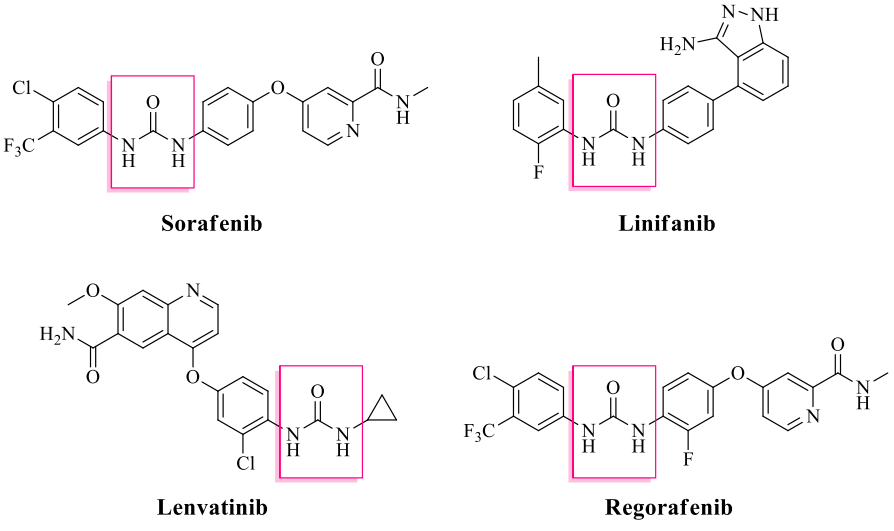

Fig. 1 Several drugs containing urea moiety with antiproliferative activity

it can block the Raf/MEK/ERK signaling pathway, but also can inhibit more kinases involved in tumor angiogenesis and proliferation, such as VEGFR-2, PDGFR, Flit-3, and c-KIT [26].

The method of this work is to dimerize part of the molecular structure of sorafenib, which has been confirmed as a potential target based on in silico studies. For this suggestion, a variety of linkers such as aromatic and aliphatic groups were used to connect the urea moieties.

Results and discussion

Chemistry

Conferring on in silico analyses and docking studies on sorafenib drug concluded that unit of [1-(4-chloro-3-(trifluoromethyl)phenyl)-3-urea-] is the core active site. This active site encouraged us to synthesize *bis*-urea compound that contains two urea units in its structure. Based on our previous works related to the two-directional synthesis, and with a focus on exploring convenient synthetic methods for the production of compounds with pharmacological activities [27–35], a one-pot 3-CR for the preparation of *bis*-urea scaffolds (Scheme 1) from the reaction of 2 eq. isocyanate derivatives **1** to 1 eq. of diamino-compounds **2** was developed. A total of seven new *bis*-urea derivatives **3a–g** were designed, synthesized, isolated, purified, and characterized.

All compounds described in Scheme 1 were characterized by spectroscopic methods FTIR, ^{1}H NMR, and ^{13}C NMR and elemental analysis. The FTIR spectra of *bis*-urea derivatives **3a–g** reveal the presence of carbonyl C=O stretching

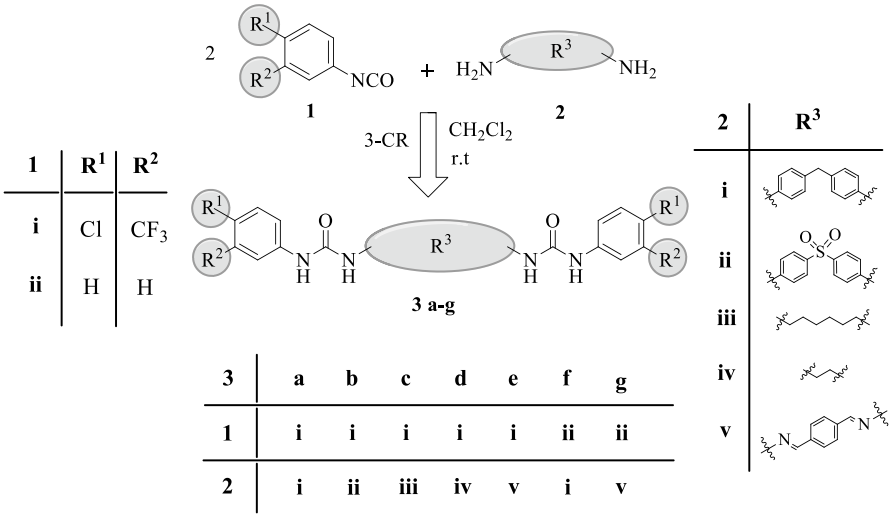

Scheme 1 Synthesis of *bis*-urea derivatives **3a–g**

vibration bands at υ 1639–1696 cm^{-1}, absorption bands in the 3277–3389 cm^{-1} and 1536–1566 cm^{-1} regions corresponding to N–H stretching and bending peaks, respectively, due to urea formation.

The ^{1}H NMR spectra of *bis*-ureas **3a–g** showed sharp bands at δ 6.5–9.5 ppm attributed to the N–H proton of urea moiety. Aromatic ring protons were observed in the expected chemical shift region and exhibited the estimated integral values for all compounds. Chemical shifts and the integral values of aliphatic protons in **3a**, **3c**, **3d**, and **3f** referred to their structures. The ^{13}C NMR spectra of *bis*-ureas **3a–g** showed signals at 152.77–155.66 ppm assigned to the carbonyls of urea groups. The carbon of CF_3 substituent displayed signals at 119–128 ppm as a quartet with $^{1}J_{FC}$ = 271–272 Hz for compounds **3a–e**. The coupling of fluorine with the second carbon ($^{2}J_{FC}$) was observed in **3b–e** as a small quartet with *J* value 30 Hz (Fig. 2; Table 1). Signals related to aromatic and aliphatic carbons resonate at their predicted locations (see the "Supplementary material" file).

The **3a**–**g** were designed and synthesized based on the predicted active sites and stabilized their molecular structure in the field of energy minimization using HyperChem software and using NCBI PubChem [36]. The importance of each portion of the molecule in relation to the properties of sorafenib as typical urea analog drug was investigated (Fig. 1). The structure of the synthesized compounds is described in Table 1.

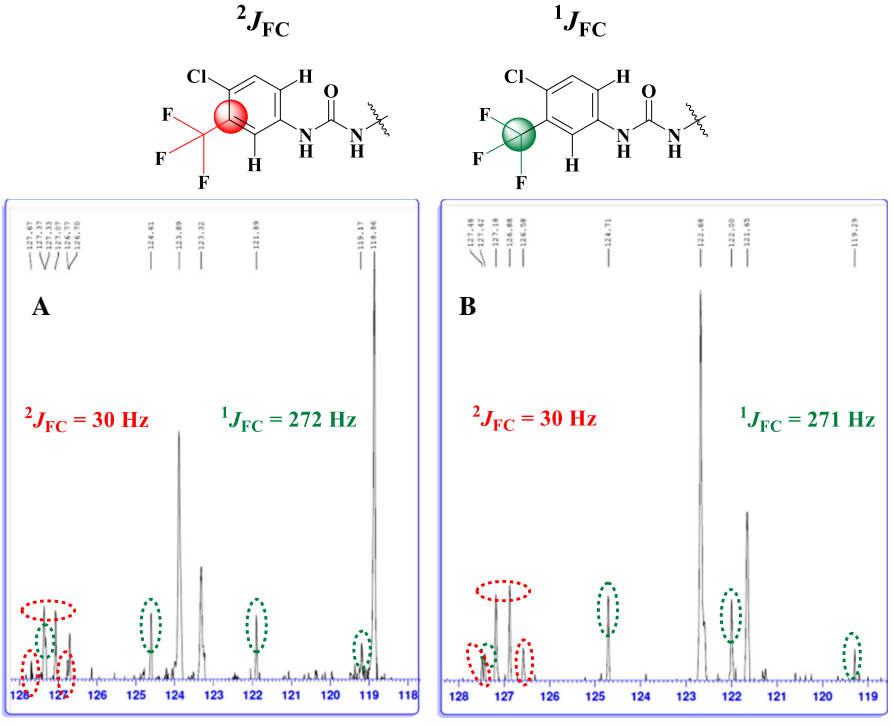

Fig. 2 Splitting patterns of $^{1}J_{FC}$ and $^{2}J_{FC}$ in ^{13}C NMR for **a 3b** and **b 3c**

Table 1 Synthesis of *bis*-urea derivatives **3a–g** with five different linkers

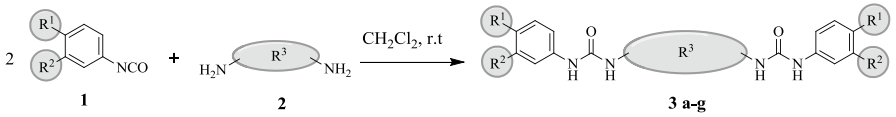

Entry	Product	Name	Time (h)	Yield[a] (%)
1	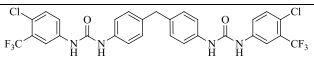	**3a**	12	90
2	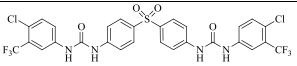	**3b**	15	86
3	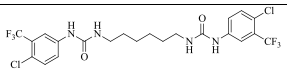	**3c**	15	88
4	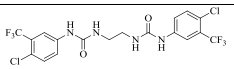	**3d**	15	85
5	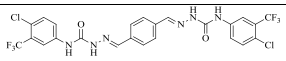	**3e**	14	80
6	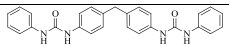	**3f**	12	86
7	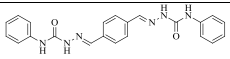	**3g**	14	84

All of the reactions were carried out with **1** (9.6 mmol) and **2** (4.5 mmol) in CH_2Cl_2 (8 + 8 mL)

[a]Isolated yield

Biology

In silico analyses

According to Lipinski's Rule of Five [37], 74 analogs are designed to find better compounds than the structure of sorafenib as typical urea analog drugs. As a first step, these analogs were made by little in silico modifications. Substitute groups included are OH, CH_3, Cl, NH_2, cyclopentane, and pyrrole.

The results showed that for minor modification, the best potential atoms of sorafenib might be N11 and C23.

The results of this analysis are used to potentially initiate the main research idea for the synthesis of new compounds with further modifications of sorafenib. (For more information, please see the "Supplementary material" file, in particular, Figs. S1 and S2.)

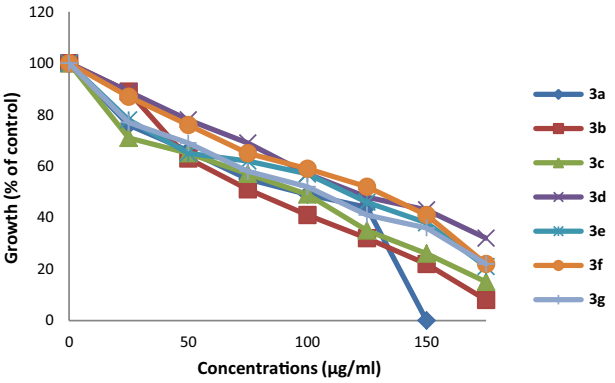

Fig. 3 Antiproliferative activity of compounds **3a–g** against HT-29 cells using MTT assays

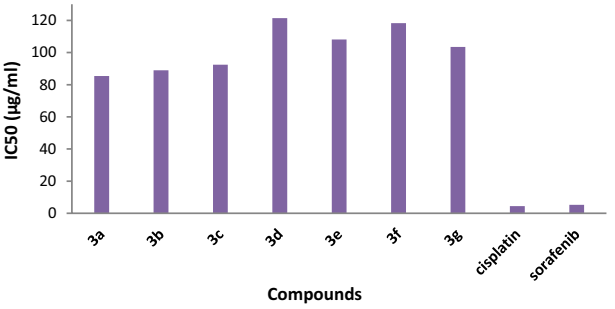

Fig. 4 IC_{50} values of derivatives **3a–g**, sorafenib and cisplatin against the HT-29 cells

Cytotoxic activity

In the present work, we investigated the cytotoxic effects of **3a–g** on human colon adenocarcinoma cell line proliferation (HT-29) and human normal adult dermal fibroblasts (HDF). Cells were treated with different concentrations of the **3a–g**, sorafenib, and cisplatin in different amounts ranging from 0 to 175 µM for 24 h. Cells were incubated with **3a–g** and cell viability was measured 18 h later by MTT assay. Inhibition of cell proliferation in each treatment is reported as a percentage of the number of cells treated in relation to the untreated control cells (Fig. 3). Figure 4 shows the IC_{50} values of **3a–g**. The IC_{50} of cisplatin and sorafenib, as the positive control group, under all identical conditions, was approximately 4.49 and 5.25 µM, respectively. MTT assay results showed that **3a** had higher cytotoxicity than other compounds. However, all IC_{50} values showed approximately reasonable activity for the compounds. Among the compounds tested, **3a**, **3b**, and **3c** exhibited antiproliferative activity with $\mathbf{IC_{50}}$ of 85.37, 88.92, and 92.46 µM, respectively.

Relatively, a higher IC_{50} value (> 450 μM) for **3a–g** on the normal fibroblast cells compared to the colon adenocarcinoma cells of HT29 indicates that the **3a–g** are nontoxic to normal human cells.

It appears that the presence of substituents in the phenyl rings led to changes in activity. As shown, chlorine and trifluoromethyl substituents, similar in structure to sorafenib, are effective in the activity of **3a–e** compared to positive control groups (cisplatin and sorafenib). However, in the case of **3d**, it seems that decreasing the length of the linkage between two urea moieties resulted in decreased activity.

Antibacterial activity

The in vitro antibacterial activities of compounds were measured against Gram-negative (GN) and Gram-positive (GP) bacteria. Four standard microorganisms were used: *Escherichia coli* (*E. coli*) and *Pseudomonas aeruginosa* (*P. aeruginosa*) as GN; and *Staphylococcus aureus* (*S. aureus*) and *Micrococcus luteus* (*M. luteus*) as GP. The results are reported in Table 2. As shown, most of the compounds exhibit strong activities toward GP bacteria (*Micrococcus luteus* and *Staphylococcus aureus*) and no reactivity was found against GN bacteria. Changes in activity are due to the effect of substituents on the phenyl ring. As shown, compounds **3f** and **3g** showed no activity in either bacterial group. The presence of Cl and CF_3 is highly effective in the antibacterial activity of **3a–e** in comparison with the positive controls (ciprofloxacin and ampicillin).

GN bacteria are surrounded by a thin murein cell wall that is surrounded by an outer membrane containing lipopolysaccharide. GP bacteria lack the outer membrane but are often surrounded by murein layers thicker than those found in GN ones. As can be seen, *S. aureus* and *M. luteus* were generally sensitive, unlike two

Table 2 Antibacterial activity of the compounds (**3a–g**)

Entry	Compound	Antibacterial activity (zone of inhibition in mm)			
		Gram-negative		Gram-positive	
		E. coli	*P. aeruginosa*	*S. aureus*	*M. luteus*
1	**3a**	–	–	14	17
2	**3b**	–	–	15	21
3	**3c**	–	–	17	14
4	**3d**	–	–	18	24
5	**3e**	–	–	20	25
6	**3f**	–	–	–	–
7	**3g**	–	–	–	–
8	Ciprofloxacin[a]	13	28	13	11
9	Ampicillin[a]	8	–	22	27
10	DMSO[b]	–	–	–	–

[a]Positive control

[b]Negative control

GN isolates. However, the synthesized compounds displayed great activity on this bacterium relative to positive controls. This may be explained by the fact that although some transport mechanisms in cell membranes are quite general, others require specific proteins for transportation to take place. In general, due to the presence of the two distinct membranes in GN bacteria, they are more effective in expelling harmful molecules, or inhibiting their entry into the cytosol. The order of increased activity **3c**, **3d**, and **3e** exhibited strong activities against *S. aureus*, and **3a**, **3b**, **3d**, and **3e** showed strong activity against *M. luteus*.

Conclusions

In conclusion, a new and efficient one-pot 3MCR based on the in silico analyses for the synthesis of *bis*-urea compounds from a variety of diamino-substituted derivatives and isocyanate derivatives at r.t. with good yields was developed. The di-substituted aryl urea residue similar to the part of the molecular structure of sorafenib is practically present in **3a–g** products. Simplicity, easy execution, high atom economy, simple workup and good yields are aspects of this synthetic procedure. In vitro antibacterial activity of the compounds showed that the presence of Cl and CF_3 substitutions is very effective in the high activity of compounds in comparison with positive controls. The cytotoxic effects of compounds against the HT-29 colorectal cell line using a modified MTT assay are studied. The presence of substituents in phenyl rings and the use of different linkers result in a change in activity.

Experimental section

Chemistry

Materials and methods

Chemical materials were purchased from Aldrich, Merck, and Fluka and were used without further purification. The purity definition of the substrate and reaction monitoring were done using thin-layer chromatography (TLC) on silica-gel polygram SILG/UV 254 plates. The FTIR spectra were determined on a Shimadzu IR-470 spectrometer. Melting points were recorded on a Büchi B-545 apparatus in open capillary tubes and are uncorrected. All ^{1}H NMR and ^{13}C NMR data were recorded using a Bruker Avance 400 and 100-MHz spectrometer at 293 K and dimethyl sulfoxide (DMSO)-d6, and spectra were internally referenced to tetramethylsilane (TMS). Chemical shifts are reported in ppm (δ) using deuterated solvents as internal references. Elemental analysis was made by a Carlo-Erba EA1110 CNNO-S analyzer and agreed with the calculated values.

General procedure for the synthesis of *bis*-urea derivatives (3a–g)

Appropriate derivatives of diamino-substituted compounds (**2**, 4.5 mmol, 1 eq) were dissolved in CH_2Cl_2 (8 mL) at r.t. A solution of isocyanate derivatives (**1**, 9.6 mmol, 2.05 eq) in CH_2Cl_2 (8 mL) was added dropwise to the mixture under vacuum/argon condition. The mixture was stirred at r.t. for a period of times as shown in Table 1; the reaction progress was monitored by TLC. Then, the reaction mixture was filtered and washed with CH_2Cl_2 (2 mL × 2) to result in the compounds (**3a–g**) as powdered solid yields shown in Table 1. The products were established by their ^{1}H NMR, ^{13}C NMR, FTIR, and elemental analysis data.

1,1′-(Methylenebis(4,1-phenylene))bis(3-(4-chloro-3-(trifluoromethyl)phenyl) urea) (3a) Creamy powder, yield 90%. Mp: 244–247 °C. ^{1}H NMR (400 MHz, DMSO) (δ/ppm): 9.12 (2H, s, N–H), 8.77 (2H, s, N–H), 8.11 (2H, s, Ar–H), 7.62 (4H, m, Ar–H), 7.38 (4H, d, J = 8.4 Hz, Ar–H), 7.15 (4H, d, J = 8.4 Hz, Ar–H), 3.84 (2H, s, –CH_2–). ^{13}C NMR (100 MHz, DMSO) (δ/ppm): 152.57 (C=O of urea), 119.24–127.39 (q, $^1J_{FC}$ = 272 Hz, –CF_3), 118.91–139.34 (Ar–C), 40.06 (–CH_2–). IR (ν_{max}/cm^{-1}): 1647 (C=O stretching), 3277 (N–H stretching), 1552 (N–H bending). Anal Calcd. for $C_{29}H_{20}Cl_2F_6N_4O_2$: C, 54.31; H, 3.14; N, 8.74%. Found C, 54.33; H, 3.11; N, 8.70%; exact mass: (M^+): Calcd 640.0868; found 640.0871.

1,1′-(Sulfonylbis(4,1-phenylene))bis(3-(4-chloro-3-(trifluoromethyl)phenyl)urea) (3b) White powder, yield 86%. Mp: 175–178 °C. ^{1}H NMR (400 MHz, DMSO) (δ/ppm): 9.39 (2H, s, N–H), 9.31 (2H, s, N–H), 8.11 (2H, s, Ar–H), 7.86 (2H, d, J = 8.8 Hz, Ar–H), 7.76 (2H, d, J = 8.8 Hz, Ar–H), 7.69 (4H, d, J = 8.8 Hz, Ar–H), 7.62–7.65 (4H, m, Ar–H). ^{13}C NMR (100 MHz, DMSO) (δ/ppm): 152.63 (C=O of urea), 126.77–127.67 (q, $^2J_{FC}$ = 30 Hz, –C–CF_3), 119.17–127.33 (q, $^1J_{FC}$ = 272 Hz, –CF_3), 118.86–139.34 (Ar–C). IR (ν_{max}/cm^{-1}): 1665 (C=O stretching), 3338 (N–H stretching), 1544 (N–H bending). Anal Calcd. for $C_{28}H_{18}C_{l2}F_6N_4O_4S$: C, 48.64; H, 2.62; N, 8.10%. Found C, 48.61; H, 2.61; N, 8.14%. Exact mass: (M^+): Calcd 690.0330; found 690.0328.

1,1′-(Hexane-1,6-diyl)bis(3-(4-chloro-3-(trifluoromethyl)phenyl)urea) (3c) White powder, yield 88%. Mp: 189–192 °C. ^{1}H NMR (400 MHz, DMSO) (δ/ppm): 8.95 (2H, s, N–H), 8.07 (2H, d, $^4J_{HH}$ = 2.4 Hz, Ar–H), 7.57 (2H, dd, J = 8.8 Hz, $^4J_{HH}$ = 2.4 Hz, Ar–H), 7.53 (2H, d, J = 8.8 Hz, Ar–H), 6.35 (2H, t, $^3J_{H–N–C–H}$ = 5.6 Hz, N–H), 3.07–3.12 (4H, m, –CH_2–), 1.43–1.45 (4H, m, –CH_2–), 1.31–1.32 (4H, m, –CH_2–). ^{13}C NMR (100 MHz, DMSO) (δ/ppm): 155.33 (C=O of urea), 126.58–127.48 (q, $^2J_{FC}$ = 30 Hz, –C–CF_3), 119.29–127.42 (q, $^1J_{FC}$ = 271 Hz, –CF_3), 116.47–140.70 (Ar–C), 26.56–31.17 (–CH_2–). IR (ν_{max}/cm^{-1}): 1651 (C=O stretching), 3324 (N–H stretching), 1566 (N–H bending). Anal Calcd. for $C_{22}H_{22}C_{l2}F_6N_4O_2$: C, 47.24; H, 3.96; N, 10.02%. Found C, 47.20; H, 3.95; N, 10.06%. Exact mass: (M^+): Calcd 558.1024; found 558.1018.

1,1′-(Ethane-1,2-diyl)bis(3-(4-chloro-3-(trifluoromethyl)phenyl)urea) (3d) White powder, yield 85%. Mp: 192–194 °C. ^{1}H NMR (400 MHz, DMSO) (δ/ppm): 9.29 (2H, s, N–H), 8.08 (2H, d, $^{4}J_{HH}$ = 2.4 Hz, Ar–H), 7.58 (2H, dd, J = 9.0 Hz, $^{4}J_{HH}$ = 2.4 and 2.0 Hz, Ar–H), 7.53 (2H, d, J = 8.8 Hz, Ar–H), 6.60 (2H, s, N–H), 3.21–3.23 (4H, m, –CH_2–). ^{13}C NMR (100 MHz, DMSO) (δ/ppm): 155.66 (C=O of urea), 126.57–127.47 (q, $^{2}J_{FC}$ = 30 Hz, –C–CF_3), 119.28–127.41 (q, $^{1}J_{FC}$ = 271 Hz, –CF_3), 116.54–140.67 (Ar–C), 35.63 (–CH_2–). IR (ν_{max}/cm^{-1}): 1646 (C=O stretching), 3333 (N–H stretching), 1565 (N–H bending). Anal Calcd. for $C_{18}H_{14}C_{l2}F_6N_4O_2$: C, 42.96; H, 2.80; N, 11.13%. Found C, 42.99; H, 2.78; N, 11.14%. Exact mass: (M^+): Calcd 502.0398; found 502.0392.

(2E,2′E)-2,2′-(1,4-Phenylenebis(methanylylidene))bis(*N*-(4-chloro-3-(trifluoromethyl)phenyl)hydrazinecarboxamide) (3e) Pale yellow powder, yield 80%. Mp: 289–291 °C. ^{1}H NMR (400 MHz, DMSO/Acetone 1:1) (δ/ppm): 11.10 (2H, s, N–H), 9.42 (2H, s, N–H), 8.37 (2H, d, $^{4}J_{HH}$ = 2.4 Hz, Ar–H), 8.12 (2H, d, J = 8.8 Hz, $^{4}J_{HH}$ = 2.0 Hz, Ar–H), 8.07 (2H, s, HC = N), 7.89–7.97 (4H, m, Ar–H), 7.65 (2H, d, J = 8.8 Hz, Ar–H). ^{13}C NMR (100 MHz, DMSO/Acetone 1:1) (δ/ppm): 153.77 (C=O of urea), 141.83 (–C=N–), 127.11–128.02 (q, $^{2}J_{FC}$ = 30.5 Hz, –C–CF_3), 119.70–127.83 (q, $^{1}J_{FC}$ = 271 Hz, –CF_3), 119.21–139.84 (Ar–C). IR (ν_{max}/cm^{-1}): 1696 (C=O stretching), 3389 (N–H stretching), 1536 (N–H bending). Anal Calcd. for $C_{24}H_{16}C_{l2}F_6N_6O_2$: C, 47.62; H, 2.66; N, 13.88%. Found C, 47.60; H, 2.65; N, 13.83%. Exact mass: (M^+): Calcd 604.0616; found 604.0611.

1,1′-(Methylenebis(4,1-phenylene))bis(3-phenylurea) (3f) White powder, yield 86%. Mp: > 300 °C. ^{1}H NMR (400 MHz, DMSO) (δ/ppm): 9.42 (2H, s, N–H), 8.80 (2H, s, N–H), 7.97 (4H, d, J = 8.8 Hz, Ar–H), 7.72–7.78 (2H, m, Ar–H), 7.58 (4H, d, J = 8.4 Hz, Ar–H), 7.10–7.18 (4H, m, Ar–H), 6.72–6.89 (4H, m, Ar–H), 3.83 (2H, s, –CH_2–). ^{13}C NMR (100 MHz, DMSO) (δ/ppm): 153.69 (C=O of urea), 120.91–138.07 (Ar–C), 44.26 (–CH_2–). IR (ν_{max}/cm^{-1}): 1639 (C=O stretching), 3303 (N–H stretching), 1558 (N–H bending). Anal Calcd. for $C_{27}H_{24}N_4O_2$: C, 74.29; H, 5.54; N, 12.84%. Found C, 74.30; H, 5.51; N, 12.82%. Exact mass: (M^+): Calcd 436.1899; found 436.1904.

(2E,2′E)-2,2′-(1,4-Phenylenebis(methanylylidene))bis(*N*-phenylhydrazinecarboxamide) (3g) Lemon yellow powder, yield 84%. Mp: > 300 °C. ^{1}H NMR (400 MHz, DMSO) (δ/ppm): 10.86 (2H, s, N–H), 10.12 (2H, s, N–H), 8.68 (2H, s, HC=N), 8.00 (4H, s, Ar–H), 7.47 (4H, d, J = 7.6 Hz, Ar–H), 7.27–7.34 (4H, m, Ar–H), 6.98 (2H, t, J = 7.4 Hz, Ar–H). ^{13}C NMR (100 MHz, DMSO) (δ/ppm): 153.01 (C=O of urea), 145.25 (–C=N–), 118.65–140.19 (Ar–C). IR (ν_{max}/cm^{-1}): 1677 (C=O stretching), 3362 (N–H stretching), 1541 (N–H bending). Anal Calcd. for $C_{22}H_{20}N_6O_2$: C, 65.99; H, 5.03; N, 20.99%. Found C, 66.02; H, 5.06; N, 20.97%. Exact mass: (M^+): Calcd 400.1648; found 400.1646.

Biology

In silico analyses

The molecular structure of sorafenib was obtained from NCBI PubChem [36] and then stabilized regarding energy minimization by HyperChem software. Based on the predicted active sites, the grid box was designed for every six candidate receptors as $100 \times 100 \times 100$ for XYZ. The in silico results indicated no remarkable candidate among 74 in silico synthesized analogs from sorafenib. The results demonstrated that little alterations make no difference in sorafenib analogs to bind more powerful with their targets compared to sorafenib. (For more information, please see the "Supplementary material" file, in particular, Figs. S1 and S2.)

Cytotoxic activity

Cell culture The human colon adenocarcinoma (HT-29) cell line and normal human adult dermal fibroblasts (HDF) were obtained from the Pasteur Institute of Iran (Tehran, I.R. Iran). The cells were maintained at 37 °C in a humidified atmosphere (90%) containing 5% CO_2 and then cultured in DMEM (Dulbecco's Modified Eagle's Medium) with 10% (v/v) FBS (fetal bovine serum), 100 units/mL penicillin, and 100 µM streptomycin. The cells were seeded overnight and then incubated with different concentrations of the **3a–g**, sorafenib, and cisplatin.

Cell viability The cell viability was determined using a modified MTT (3-(4,5-dimethylthiazol-2-y1)-2,5-diphenyltetrazolium bromide) assay [38]. In brief, the cells (1×104 cells/well) were seeded in 96-well plates and exposed to the indicated concentration of the **3a–g**, sorafenib, and cisplatin for 24 h. The samples including **3a–g**, sorafenib, and cisplatin were tested at 25, 50, 75, 100, 125, 125, 150, 150, and 175 µM concentrations. The samples were dissolved in dimethyl sulfoxide (DMSO) and further diluted with cell culture medium. The final concentration of DMSO was adjusted to 1% of the total volume of the medium in all treatment, including the blank. A control medium without DMSO was also incubated. After the treatment, 5 mg/mL of MTT solution was added and incubated for 3 h at 37 °C in a dark place. The absorbance of formazan creation was measured at a wavelength of 540 nm with an enzyme-linked immunosorbent assay (ELISA) reader (Molecular Devices, Sunnyvale, CA, USA). The cell viability by MTT assay was calculated as a percentage of the control value (untreated cells) (Fig. 3).

Antibacterial activity

Antibacterial activity was determined using the good diffusion technique; 50 µl of bacterial culture, grown in nutrient broth (*Merck*) overnight at 37 °C, was inoculated onto nutrient agar (*Merck*) plates. Wells, which are 0.5 mm in diameter, were bored in the agar using the ends of sterile Pasteur pipettes; 0.2 mg of samples was dissolved in 0.2 mL DMSO to a final concentration of 1 mg/mL. To each well, 30 µl of each sample was added and the plates were incubated at 37 °C overnight. For

comparison, ciprofloxacin and ampicillin were used as positive controls and DMSO as a negative control. Zones of growth inhibition were measured and the results are presented in Table 2.

Acknowledgements The authors are grateful to the Research Council of the University of Guilan for financial support of this research work.

Compliance with ethical standards

Conflict of interest There are no conflicts of interest to declare.

References

1. R. Hili, A.K. Yudin, Nat. Chem. Biol. **2**, 284 (2006)
2. K. Shin, H. Kim, S. Chang, Acc. Chem. Res. **48**, 1040 (2015)
3. E.A. Terefenko, J. Kern, A. Fensome, Bioorg. Med. Chem. Lett. **15**, 3600 (2005)
4. Q. Li, T.M. Li, K.W. Woods, Bioorg. Med. Chem. Lett. **15**, 2918 (2005)
5. A.Y. Guan, C.L. Liu, X.P. Yang, M. Dekeyser, Chem. Rev. **114**, 7079 (2014)
6. M. Wang, S. Xu, H. Lei, C. Wang, Z. Xiao, S. Jia, J. Zhi, P. Zheng, W. Zhu, Bioorg. Med. Chem. **25**, 5754 (2017)
7. D. Moreno, B. Díaz de Greñu, B. García, S. Ibeas, T. Torroba, Chem. Commun. **48**, 2994 (2012)
8. C.R. Zhao, R.Q. Wang, G. Li, X.X. Xue, C.J. Sun, X.J. Qu, W.B. Li, Bioorg. Med. Chem. Lett. **23**, 1989 (2013)
9. L. Ren, N. Jiao, Chem. Commun. **50**, 3706 (2014)
10. M.M. Gamal El-Din, M.I. El-Gamal, M.S. Abdel-Maksoud, K.H. Yoo, C.H. Oh, Eur. J. Med. Chem. **119**, 122 (2016)
11. J. Zhu, H. Bienayme, *Multicomponent Reactions* (Wiley, Weinheim, 2005), pp. 199–223
12. J.D. Sunderhaus, S.F. Martin, Chem. Eur. J. **15**, 1300 (2009)
13. I. Ugi, Pure Appl. Chem. **73**, 187 (2001)
14. M. Syamala, Org. Prep. Proced. Int. **41**, 1 (2009)
15. B. Jiang, L.Y. Xue, X.H. Wang, M.S. Tu, Y.P. Liu, S.J. Tu, Tetrahedron Lett. **53**, 1261 (2012)
16. M. Sarohaa, J.M. Khurana, New J. Chem. **43**, 8644 (2019)
17. S.S. Sajadikhah, M.T. Maghsoodlou, N. Hazeri, S. Mohamadian-Souri, Res. Chem. Intermed. **42**, 2805 (2016)
18. I. Ryu, H. Kuriyama, S. Minakata, M. Komatsu, J.Y. Yoon, S. Kim, J. Am. Chem. Soc. **121**, 12190 (1999)
19. S. Srivastava, New J. Chem. **43**, 6469 (2019)
20. A. Farhadi, J. Noei, R.H. Aliyari, M. Albakhtiyari, M.A. Takassi, Res. Chem. Intermed. **42**, 1401 (2016)
21. A. Jemal, F. Bray, M.M. Center, J. Ferlay, E. Ward, D. Forman, CA Cancer J. Clin. **61**, 69 (2011)
22. Sorafenib, BAY43-9006 (Nexavar®, Bayer) NDA 21923 Medical Review, FDA (2005)
23. Nexavar® (Sorafenib) Scientific Discussion EMEA WC500027707 (2007)
24. L. Liu, Y. Cao, C. Chen, X. Zhang, A. McNabola, D. Wilkie, S. Wilhelm, M. Lynch, C. Carter, Cancer Res. **66**, 11851 (2006)
25. G. Ranieri, G. Gadaleta-Calodarola, V. Goffredo, R. Patruno, A. Mangia, A. Rizzo, R.L. Sciorsci, C.D. Gadaleta, Curr. Med. Chem. **19**, 938 (2012)
26. S.M. Wilhelm, L. Adnane, P. Newell, A. Villanueva, J.M. Llovet, M. Lynch, Mol. Cancer Ther. **7**, 3129 (2008)
27. N.O. Mahmoodi, S. Shoja, K. Tabatabaeian, B. Sharifzadeh, Ultrason. Sonochem. **23**, 31 (2015)
28. N.O. Mahmoodi, S. Shoja, B. Sharifzadeh, M. Rassa, Med. Chem. Res. **23**, 1207 (2014)
29. R. Sharifi Aliabadi, N.O. Mahmoodi, J. Clean. Prod. **179**, 235 (2018)
30. R. SharifiAliabadi, N.O. Mahmoodi, H. Ghafoori, H. Roohi, V. Pourghasem, Res. Chem. Intermed. **44**, 2999 (2018)
31. N.O. Mahmoodi, B. Khalili, O. Rezaeianzade, A. Ghavidast, Res. Chem. Intermed. **42**, 6531 (2016)

32. N.O. Mahmoodi, I. Nikokar, M. Farhadi, A. Ghavidast, Z. Naturforsch. **B 69**, 715 (2014)
33. N.O. Mahmoodi, M. Namroudi, F. Ghanbari Pirbasti, H. Roohi, I. Nikokar, Res. Chem. Intermed. **42**, 3625 (2016)
34. N.O. Mahmoodi, N.K. Ahmadi, A. Ghavidast, J. Mol. Struct. **1160**, 463 (2018)
35. A. Sheykhi-Estalkhjani, N.O. Mahmoodi, A. Yahyazadeh, M. Pasandideh Nadamani, Tetrahedron **74**, 4868 (2018)
36. https://pubchem.ncbi.nlm.nih.gov/compound/216239
37. C.A. Lipinski, F. Lombardo, B.W. Dominy, P.J. Feeney, Adv. Drug Deliv. Rev. **64**, 4 (2012)
38. M.V. Berridge, P.M. Herst, A.S. Tan, Biotechnol. Annu. Rev. **11**, 127 (2005)

Affiliations

Sajede Shoja[1] · Nosrat Ollah Mahmoodi[1] · Hossein Ghafouri[2] · Mehdi Rassa[2] · Alireza Sharafshah[3] · Esmaeel Panahi Kokhdan[4]

✉ Nosrat Ollah Mahmoodi
mahmoodi@guilan.ac.ir

[1] Department of Chemistry, Faculty of Sciences, University of Guilan, PO Box 41335-1914, Rasht, Islamic Republic of Iran

[2] Department of Biology, Faculty of Sciences, University of Guilan, PO Box 41335-1914, Rasht, Islamic Republic of Iran

[3] Cellular and Molecular Research Center, School of Medicine, Guilan University of Medical Sciences, Rasht, Islamic Republic of Iran

[4] Medicinal Plants Research Center, Yasuj University of Medical Sciences, Yasuj, Islamic Republic of Iran